PROCEEDINGS OF SCIENCE

Other Top Quark Properties in ATLAS

Antonio Limosani*
On behalf of the ATLAS Collaboration
University of Melbourne
E-mail: antonio.limosani@cern.ch

We report on the measurements of the top quark charge and radiative top quark pair production cross section in pp collisions at $\sqrt{s} = 7$ TeV using 0.70 fb^{-1} and 1.04 fb^{-1} of data taken with the ATLAS detector at the LHC, respectively. The top quark charge is confirmed to be $+2/3e$ as expected within the Standard Model. The cross section times branching ratio for $t\bar{t}\gamma$ production with a photon with transverse momentum above 8 GeV is measured to be 2.0 ± 0.5 (statistical) ± 0.7 (systematic) ± 0.18 (luminosity) pb.

36th International Conference on High Energy Physics,
July 4-11, 2012
Melbourne, Australia

*Speaker.

PoS(ICHEP2012)203

The top quark was discovered at the Tevatron almost twenty years ago [1] yet still many of its properties have yet to be measured precisely. The increased production cross-section of top quarks at the LHC compared to that at the Tevatron will eventually allow for higher precision studies and measurements of relatively rare top quark phenomena. Here we report on two measurements performed by ATLAS at the LHC that are significant steps toward that program, namely, the measurement of the top quark charge and a measurement of top-quark pair production with a photon in the final state. The main motivation of these measurements is to confirm the standard model nature of the top quark. For example it is conceivable that the particle we call the top quark could in fact be an exotic type particle with charge -4/3e [2]. The charge can be directly inferred from its decay products or through its coupling to photon radiation. The cross section for the process $pp \to t\bar{t}\gamma$ and the confirmation of the standard model top quark charge are properties that can be determined with relatively small datasets. The $t\bar{t}\gamma$ measurement presented here does not distinguish between radiative top quark production and decay. Consequently, non-negligible interference effects between the two processes are taken into account. Both of the measurements have been described in detail in conference notes [3, 4]. What follows is a brief summary of each analysis.

The two measurements are performed using data of proton on proton collisions at $\sqrt{s} = 7$ TeV collected by the ATLAS detector. The ATLAS detector is described in detail elsewhere [5]. The top quark charge measurement uses 0.70 fb^{-1} while the measurement of $t\bar{t}\gamma$ uses 1.04 fb^{-1}. The event selection is performed in the single electron and single muon event samples. The reconstruction of $t\bar{t}$ events is achieved in the *lepton plus jets* final state, where one W from the top decays leptonically while the other W from the other top decays hadronically. The reconstructed leptons include electrons and muons.

Top pair and single top events are generated using MC@NLO with the CTEQ6.6 [6] parton distribution function. These samples are then interfaced to HERWIG v6.510 [7] for the parton shower while JIMMY [8] is used for the underlying event. The $t\bar{t}$ cross section is normalised to the approximate next-to-next-to-leading order (NNLO) prediction of 164.6 pb, obtained using the HATHOR tool [9].The single top production cross sections are normalised to the approximate NNLO prediction for the t, s and Wt production channels respectively [10]. Vector boson production is simulated using ALPGEN [11] and interfaced to HERWIG v6.510 [7] for the parton shower while JIMMY [8] is used for the underlying event. For both the matrix element calculations and the parton shower evolution the CTEQ6.1 [6] parton distribution function is used. The $t\bar{t}\gamma$ sample is generated with the WHIZARD [12] MC generator, which allows for a full calculation taking into account all possible contributing diagrams at leading order (LO).

1. Common Object and Event Selection

Electron candidates are defined as energy deposits in the electromagnetic calorimeter with an associated measured track in the inner detector. All electron candidates are required to have a transverse momentum $p_{\mathrm{T}} > 25$ GeV and $|\eta_{cl}| < 2.47$, where η_{cl} is the pseudorapidity of the electromagnetic cluster associated with the electron. Candidates in the calorimeter transition region $1.37 < |\eta_{cl}| < 1.52$ are excluded. Muon candidates are reconstructed from track segments in the different layers of the muon chambers. These segments are combined starting from the outermost layer, with a procedure that takes material effects into account, and matched with tracks found

in the inner detector. The final candidates are required to satisfy $p_{\mathrm{T}} > 20$ GeV and $|\eta| < 2.5$. Isolation criteria are used to reduce the background from hadrons mimicking lepton signatures and from decays of heavy quarks inside jets. The total energy in a cone of $\Delta R = 0.2$ around the electron candidate must not exceed 3.5 GeV, after correcting for energy deposits from pile-up. The sum of track transverse momenta and the total energy deposited in a cone of $\Delta R = 0.3$ around the muon are both required to be less than 4 GeV. Jets are reconstructed with the anti-kt algorithm (with distance parameter $R = 0.4$) starting from energy clusters of adjacent calorimeter cells. These jets are calibrated by first correcting the jet energy using the scale established for electromagnetic objects (EM scale) and then performing a further correction to the hadronic energy scale.

Signal events in the lepton plus jets final state are characterised by the presence of an isolated high p_{T} lepton with the presence of the neutrino resulting in missing transverse energy ($E_{\mathrm{T}}^{\mathrm{miss}}$), and accompanying jets from both *b*-quarks and light quarks from the W boson decay. Events were first selected with the electron or muon trigger with a transverse energy (E_{T}) threshold of 20 GeV for electrons and 18 GeV for muons. Exactly one isolated lepton (electron or muon) with E_{T} exceeding 25 GeV (electron) or 20 GeV (muon) in the event was required and this lepton had to be matched to the object firing the lepton trigger. At least four jets with transverse momentum $p_{\mathrm{T}} > 25$ GeV and within the pseudorapidity range $|\eta| < 2.5$ were required. The $E_{\mathrm{T}}^{\mathrm{miss}}$ had to exceed 35 GeV for the events with electrons, and 20 GeV for the events with muons. To ensure a good event quality, a primary vertex containing at least five charged particles was required, and events containing jets in poorly instrumented regions with transverse momentum exceeding 20 GeV were removed. The transverse mass of the leptonically decaying W boson in the event was reconstructed as $m_{\mathrm{T}}(W) = \sqrt{p_l p_\nu (1 - cos(\phi_l - \phi_\nu))}$, where the measured $E_{\mathrm{T}}^{\mathrm{miss}}$ provided information on the transverse momentum and ϕ angle of the neutrino. For the events with electrons this mass had to exceed 25 GeV, while the sum of this mass and $E_{\mathrm{T}}^{\mathrm{miss}}$ had to exceed 60 GeV for the events with muons. Finally, at least one jet was required to be from a well-reconstructed displaced vertex, b-tag [13]. The $t\bar{t}\gamma$ measurement uses a combination of two b-tagging algorithms. One algorithm exploits the topology of weak b- and c-hadron decays inside the jet. The second one uses the transverse and the longitudinal impact parameter significances of each track within the jet to determine a likelihood that the jet originates from a b-quark. The results from both b-tagging algorithms are combined using an artificial neural network to determine a single discriminating variable which is used to make tagging decisions [14]. A cut on the neural network output is chosen such that approximately 70% of b-jets from $t\bar{t}$ decays are accepted.

2. b-quark charge measurement

The charge of the Standard Model top (or exotic) quark was determined by studying the charges of its decay products. To determine the b-jet charge, a weighting technique was employed in which the b-jet charge is defined as a weighted sum of the charges of its associated tracks:

$$Q_{b-jet} = \frac{\sum_i q_i \left| \vec{j} \cdot \vec{p}_i \right|^{\kappa}}{\sum_i \left| \vec{j} \cdot \vec{p}_i \right|^{\kappa}}, \tag{2.1}$$

Model	$\langle Q_{\rm comb} \rangle$		
	e+jets	μ+jets	combined
SM	-0.084 ± 0.020	-0.081 ± 0.023	-0.082 ± 0.020
Exotic	$+0.085 \pm 0.028$	$+0.088 \pm 0.023$	$+0.083 \pm 0.020$
Measured	-0.088 ± 0.022	-0.078 ± 0.020	-0.082 ± 0.015
Model	$\langle Q^{\rm soft}_{\rm comb} \rangle$		
	e+jets	μ+jets	combined
SM	-0.237 ± 0.016	-0.232 ± 0.015	-0.234 ± 0.011
Exotic	$+0.241 \pm 0.016$	$+0.180 \pm 0.015$	$+0.209 \pm 0.011$
Measured	-0.36 ± 0.09	-0.26 ± 0.10	-0.31 ± 0.07

Table 1: The measured and the expected average values of $Q_{\rm comb}$ and $< Q^{\rm soft}_{\rm comb} >$. The expected values are for the Standard Model top and the exotic quark scenarios. The errors on the measured values include both the statistical and the systematic uncertainties [3].

where $q_i(p_i)$ is the charge (momentum) of the $i^{\rm th}$ track, $\vec{j}$ is the b-jet axis direction and $\kappa = 0.5$ is a parameter optimized for the best separation of b and $\bar{b}$ jets. For optimal separation, ten or fewer tracks are required that have $p_{\rm T} > 10$ GeV pointing to a b-jet within a cone of $\Delta R = 0.25$. It was verified that the optimization is not very sensitive to multiple events in one beam crossing. The expression

$$Q_{\rm comb} = Q_{b-jet} \cdot Q_l$$

where Q_l, which is the lepton charge, is used to distinguish the Standard Model from the exotic scenario. The lepton and b-jet pairing was performed using the invariant mass distribution of the lepton and the b-tagged jet. The efficiency of the invariant mass criterion together with the requirement of two b-tagged jets when measured on the sample of events passing the standard semileptonic selection described previously is 9.3%.

Muons from semileptonic B-hadron decays are identified as non-isolated muons inside corresponding b-jets, and their charge have the same sign as the charge of the b quark that produced the jet. But this assignment is diluted by the presence of muons from semileptonic charm decays, which usually have the opposite charge or from B-mesons having oscillated to their charge conjugate partner before decay. A likelihood based method was used to determine the correct event topology, specifically the correct pairing of a jet (b-tagged or not) with the isolated lepton stemming from the semileptonic W decay. The selected jet was assigned to the correct lepton in 68% of events. The total selection efficiency relative to the standard semileptonic $t\bar{t}$ described previously was 4%. The variable $Q^{\rm soft}_{\rm comb} = Q_{{\rm soft}\,\mu} \cdot Q(l)$ is used to determine the top quark charge. To reduce the number of muons from charm decays a cut on the $p_{\rm T}$ of the soft muon with respect to the jet axis of 800 MeV was employed.

The values of $\langle Q^{\rm soft}_{\rm comb} \rangle$ (soft muon method) and $\langle Q_{\rm comb} \rangle$ (track charge weighting method) are shown in Table 1. The data are consistent with the Standard Model prediction.

Given the good agreement between the measurements and the Standard Model, the top quark with an exotic charge of $4/3e$ can be excluded. To quantify this exclusion a standard likelihood approach was adopted. Two hypotheses: the Standard Model (null hypothesis) where the top quark

has charge $2/3e$, and the exotic quark hypothesis, with a charge of $4/3e$, were compared. The measured $< Q_{\text{comb}} >$ and $< Q_{\text{comb}}^{\text{soft}} >$ are each more than 4.5σ away from the values expected from the exotic quark hypothesis when the two lepton flavors are treated separately. If electron and muon channels are combined, the exotic quark scenario is excluded at a confidence level greater than 5σ with either of the b-quark charge measurement methods.

3. $t\bar{t}\gamma$ measurement

On top of the selection mentioned in Section 1, additional requirements are applied to select photons. The event has to contain at least one good photon with a transverse energy of more than 15 GeV, and in the electron channel, the invariant mass of the electron and photon has to be outside of a ± 5 GeV mass window around the Z peak ($m_{e\gamma} < 86$ GeV or $m_{e\gamma} > 96$ GeV) in order to reject $Z \to e^+e^-$ events where one of the electrons is being misidentified as a photon. In the data sample used there are 52 events in the electron channel and 70 events in the muon channel that fulfil all selection criteria. From $t\bar{t}\gamma$ Monte Carlo simulation, a prediction of 22 and 28 signal events is derived in the electron and muon channel, respectively.

The efficiency times acceptance of the object and event selection is taken from the signal $t\bar{t}\gamma$ sample for both the electron and muon channel separately. In the electron channel, the efficiency times acceptance is 1.0% and in the muon channel it is 1.3% with respect to the full signal sample. This includes the branching ratio into the single electron or single muon channel of 26% and the acceptance of 58% for the photon p_{T} cut at 15 GeV with respect to the cut in the generation of the signal sample at 8 GeV.

The cross section measurement is based on a template fit method, using the track isolation p_{T}^{cone20} distributions for two different kinds of photon candidates, prompt photons and photons from the decay of hadrons (hadron fakes), e.g. jets fragmenting with a hard π^0, as the discriminating variable. The track isolation p_{T}^{cone20} is defined as the scalar sum of the transverse momenta of all tracks in a cone with $\Delta R = 0.2$ around the photon candidate. In order to measure the number of signal and background events, the template fit of all photon candidates is performed using different templates for signal-like prompt photons and hadron fakes. The track isolation distributions are obtained from data.

Fig. 1 compares the templates for prompt photons and hadron fakes. The signal template for prompt photons is obtained from $Z \to ee$ decays in data, exploiting the similar isolation shape of electrons and prompt photons. Small differences between electrons from Z decays and photons from $t\bar{t}\gamma$ decays have been found in Monte Carlo simulations. The data electron template is corrected using the extrapolation from electrons to photons obtained from Monte Carlo simulation, in bins of photon pseudorapidity and transverse momentum. The template for hadrons misidentified as photons is extracted from a data stream obtained from jet triggers by inverting at least one requirement on the shower shape variables [15].

The main background is $t\bar{t}$ events with a hadron fake. Such processes are already suppressed by the tight shower shape cuts on the photons, but remain the most sizeable background. Their contribution and those of all other processes with hadron fakes are calculated from the template fit. Another important background is events from the dileptonic decay mode of top pair production where one electron is misidentified as a photon. For top pair production the final source of back-

ground events is $t\bar{t}\gamma$ events that do not fulfil the WHIZARD phase space. Remaining background contributions include W+jets(+γ), Z+jets(+γ), diboson contributions (WW, WZ, ZZ), QCD multijet events with an additional prompt photon and a small contribution from single top quark events.

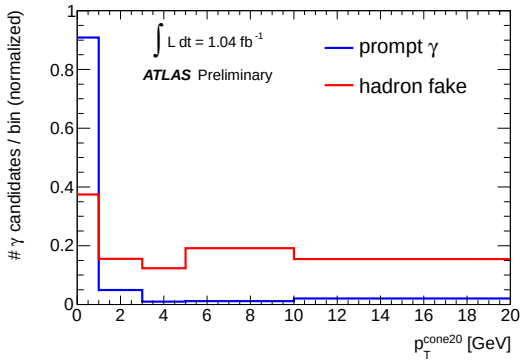

Figure 1: Templates derived from data for prompt photons (blue) and fake photons from hadrons (red), normalised to unity [4].

The total prediction of background events from Monte Carlo simulations is calculated from the sum of the radiation from muons and τ leptons and from bremsstrahlung yields $0.22^{+0.45}_{-0.22}$ events in the single electron channel and $0.4^{+0.6}_{-0.4}$ events in the single muon channel. Radiation from electrons is taken into account by the $e \to \gamma$ fake rate. This background is included in the fit using the same template as for the signal. The total background from non-$t\bar{t}$ sources, which is dominated by the inclusive boson production background is 6.7 ± 2.8 and 3.8 ± 2.1 in the electron and muon channels, respectively.

After the determination of the signal and background templates and the estimation of further background sources, the template fit is performed in both the electron and muon channel simultaneously. For the $t\bar{t}\gamma$ signal the fit yields 46 ± 12 events over a background of 78 ± 14 events. The fit result is shown in Fig. 2 separately for each channel.

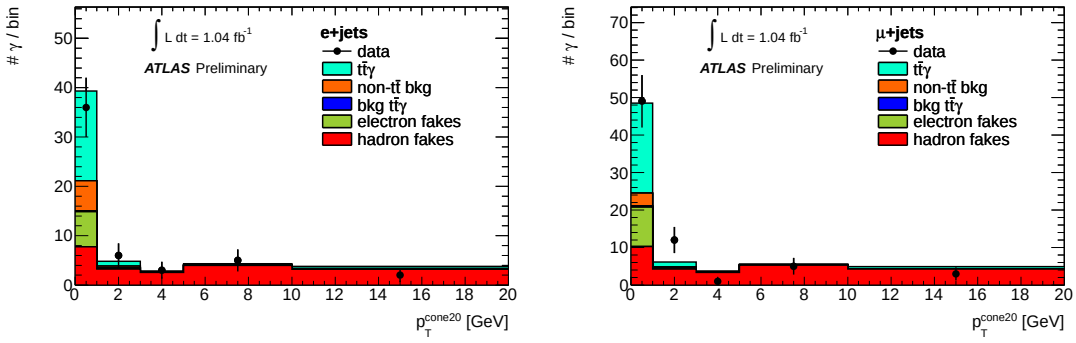

Figure 2: Result of the template fit using both channels, shown separately for the single electron channel (left) and for the single muon channel (right). The predicted $t\bar{t}\gamma$ signal is shown on top of the different background contributions [4].

The cross section times branching ratio for $t\bar{t}\gamma$ production with a photon with transverse momentum above 8 GeV is measured to be $\sigma_{t\bar{t}\gamma} \cdot \mathrm{BR} = 2.0 \pm 0.5$ (statistical) ± 0.7 (systematic) ± 0.18 (luminosity) pb.

The dominant systematic uncertainty in the $t\bar{t}\gamma$ cross section measurement originates from the estimation of the photon identification efficiency, which is based on shifts of the Monte Carlo shower shapes with respect to a candidate sample in data. The uncertainty of the efficiency includes the intrinsic precision of the method, the choice of the photon candidate sample, imperfect knowledge of the material in front of the calorimeter, the admixture of fragmentation photons and the classification of unconverted and converted photon candidates [16]. In order to test the background only hypothesis, the background expectation of 78 ± 14 events is varied according to the statistical uncertainties. The null hypothesis yields a *p*-value of 0.71%, which corresponds to a significance of 2.7 σ.

References

[1] F. Abe *et al.* [CDF Collaboration], Phys. Rev. Lett. **74**, 2626 (1995) [hep-ex/9503002]. S. Abachi *et al.* [D0 Collaboration], Phys. Rev. Lett. **74** (1995) 2632 [hep-ex/9503003].

[2] U. Baur, M. Buice and L. H. Orr, Phys. Rev. D **64** (2001) 094019 [hep-ph/0106341].

[3] ATLAS Collaboration, ATLAS-CONF-2011-141, http://cdsweb.cern.ch/record/1385517

[4] ATLAS Collaboration, ATLAS-CONF-2011-153, http://cdsweb.cern.ch/record/1398197

[5] ATLAS Collaboration, 2008 JINST 3 S08003

[6] P. M. Nadolsky, H. -L. Lai, Q. -H. Cao, J. Huston, J. Pumplin, D. Stump, W. -K. Tung and C. -P. Yuan, Phys. Rev. D **78** (2008) 013004 [arXiv:0802.0007 [hep-ph]].

[7] G. Corcella, I. G. Knowles, G. Marchesini, S. Moretti, K. Odagiri, P. Richardson, M. H. Seymour and B. R. Webber, JHEP **0101** (2001) 010 [hep-ph/0011363].

[8] J. M. Butterworth, J. R. Forshaw and M. H. Seymour, Z. Phys. C **72** (1996) 637 [hep-ph/9601371].

[9] M. Aliev, H. Lacker, U. Langenfeld, S. Moch, P. Uwer and M. Wiedermann, Comput. Phys. Commun. **182** (2011) 1034 [arXiv:1007.1327 [hep-ph]].

[10] N. Kidonakis, Phys. Rev. D **83** (2011) 091503 [arXiv:1103.2792 [hep-ph]]. Phys. Rev. D **81** (2010) 054028 [arXiv:1001.5034 [hep-ph]]. Phys. Rev. D **82** (2010) 054018 [arXiv:1005.4451 [hep-ph]].

[11] M. L. Mangano, M. Moretti, F. Piccinini, R. Pittau and A. D. Polosa, JHEP **0307** (2003) 001 [hep-ph/0206293].

[12] W. Kilian, T. Ohl and J. Reuter, Eur. Phys. J. C **71** (2011) 1742 [arXiv:0708.4233 [hep-ph]].

[13] ATLAS Collaboration, ATLAS-CONF-2010-041 (2010). http://cdsweb.cern.ch/record/1277682

[14] ATLAS Collaboration, ATLAS-CONF-2011-102. http://cdsweb.cern.ch/record/1369219

[15] Atlas Collaboration, Phys. Rev. D **83** (2011) 052005 [arXiv:1012.4389 [hep-ex]].

[16] ATLAS Collaboration, Phys. Rev. D **85** (2012) 012003 [arXiv:1107.0581 [hep-ex]].